Pseudo-First-Order Kinetic Studies of the Sorption of Acid Dyes onto Chitosan

Y. C. Wong,[1] Y. S. Szeto,[1] W. H. Cheung,[2] G. McKay[2]

[1]*Institute of Textiles, Hong Kong Polytechnic University, Hung Hom, Kowloon, Hong Kong*
[2]*Department of Chemical Engineering, Hong Kong University of Science and Technology, Clear Water Bay, Kowloon, Hong Kong*

Received 3 March 2003; accepted 25 September 2003

ABSTRACT: The adsorption of five acid dyes onto chitosan, derived through the deacetylation of crab-shell chitin, from aqueous solutions was studied. The equilibrium isotherms were measured and analyzed with the Langmuir, Freundlich, and Redlich–Peterson equations; the results correlated well with the Langmuir equation. Kinetic studies were also performed in an agitated batch adsorber to study the effect of the initial dye concentration and the mass of chitosan. The kinetics were analyzed with the pseudo-first-order rate equation, and the rate constants were determined. The first-order kinetic model correlated the experimental concentration and time data at short times and even up to 60% of the total adsorption period in a number of systems.
 J Appl Polym Sci 92: 1633–1645, 2004

Key words: adsorption; biopolymers; dyes/pigments; kinetics (polym.)

INTRODUCTION

The total dye consumption of the textile industry worldwide is in excess of 10^7 kg/year, and an estimated 90% of this ends up on fabrics. Consequently, approximately 1,000,000 kg/year of dye are discharged into waste streams by the textile industry. Dye producers and users are interested in stability and fastness and, consequently, are producing dyestuffs that are more difficult to degrade after use.[1]

In the textile sector, an estimated 10–20% of the dye (active substance) used is lost in residual liquors through exhaustion and washing operations. For pigments, the rate of loss is about 1–2%, and for paper and leather dyes, it is 10%. This amounts to about 30% of the 1,000,000,000 kg of dye consumed, as reported in 1994.[1] However, available effluent treatment processes for dye-containing effluents are currently capable of removing about half the dye lost in residual liquors. Therefore, about 400 tons daily is lost to the environment, primarily dissolved or suspended in water. Colored organic substances generally constitute only a small fraction of the total organic load in wastewater; however, their high degree of color is easily detectable and detracts from the aesthetic value of river, streams, and so forth. Therefore, as far as the public is concerned, the removal of color from wastewater is often more important than the removal of the soluble, colorless organic substances that usually contribute to the major fraction of the biochemical oxygen demand.

Industrial development is pervasively connected to the disposal of a large number of various toxic pollutants that are harmful to the environment, hazardous to human health, and difficult to degrade by natural means. The decolorization of textile wastewater is a worldwide problem to which many diverse technologies have been applied. Methods available for color removal from textile effluents are mainly divided into five categories: physical, electrochemical, photochemical, chemical, and biological treatment.[2–4]

Agricultural waste materials such as bagasse pith, sawdust, maize-cob-rich bran, rice hulls, coconut husk fibers, nut shells, and soybean and cotton seed hulls have been evaluated for their adsorption properties. These materials have been reported to adsorb different pollutants, such as heavy-metal ions, dyestuffs, and other toxic pollutants.[5–7] Sawdust waste[8] and bagasse pith[7,9,10] have been reported to be capable of adsorbing heavy-metal ions and dyestuffs from aqueous effluents.

Adsorption is a process that involves the contact of a free aqueous phase with a rigid particulate phase that has the propensity to selectively remove or store one or more solutes present in the solution.[11] Both batch-contacting and column-contacting processes are available for sorbent materials with solutions contain-

Correspondence to: G. C. McKay (kemckayg@ust.hk).
Contract grant sponsor: Research Grant Council of Hong Kong Special Administrative Region.
Contract grant sponsor: Innovation and Technology Fund of Hong Kong Special Administrative Region.
Contract grant sponsor: Hong Kong University of Science and Technology.

Journal of Applied Polymer Science, Vol. 92, 1633–1645 (2004)

TABLE I
Physical and Chemical Characteristics of Selected Dyestuffs

Generic name	Abbreviation	Commercial name	Purity (%)	Chromophore	Formula Weight	λ_{max} (nm)
C.I. Acid Green 25	AG25	Acid Green 25	75	Anthraquinone	622.6	642
C.I. Acid Orange 10	AO10	Orange G	80	Monoazo	452.4	475
C.I. Acid Orange 12	AO12	Crocein Orange G	70	Monoazo	350.3	482
C.I. Acid Red 18	AR18	New Coccine	75	Monoazo	604.5	506
C.I. Acid Red 73	AR73	Brilliant Crocein MOO	70	Diazo	566.5	510

ing dyestuffs. Liquid-phase adsorption has been shown to be an effective method for the removal of suspended solids, odors, organic matters, metal ions, and dyestuffs through the application of activated carbon,[12] peat,[13] bentonite clay, rice husk, teakwood bark, cotton waste, hair,[14,15] and maize cob[16] as adsorbents. There may be several mechanisms by which dyestuffs can be removed from a solution and attached to a sorbent particle surface. The mechanism may be due to ion exchange, physical sorption, chemisorption, chemical reactions, lone-pair-electron sharing or donating, or a number of other mechanistic processes.

Researchers have investigated adsorption systems to assess their suitability for applications in the field of water pollution control. The cost and performance of a product or the mode of application are always of concern for controlling process efficiency. Sorption equilibrium is established when the concentration of the sorbate in the bulk solution is in dynamic balance with that of the interface. An equilibrium analysis is the most important fundamental study required for evaluating the affinity or capacity of a sorbent. However, thermodynamic data can predict only the final state of a system from an initial nonequilibrium mode. It is, therefore, important to determine how sorption rates depend on the concentrations of sorbates in solutions and how rates are affected by the sorption capacity or by the character of the sorbent from a kinetic point of view. From a kinetic analysis, the solute uptake rate, which determines the residence time required for the completion of the sorption reaction, may be analyzed and established.

In this study, the ability of chitosan to remove acid dyes [Acid Green 25 (AG25), Acid Orange 10 (AO10), Acid Orange 12 (AO12), Acid Red 18 (AR18), and Acid Red 73 (AR73)] by adsorption was studied. The sorption capacities of the dyes on chitosan were studied with the adsorption isotherm technique. The experimental data were fitted to Langmuir, Freundlich, and Redlich–Peterson equations.

The sorption rates of dyestuffs onto chitosan were investigated with batch-contact-time studies. The experimental data were substituted into the pseudo-first-order reaction kinetic model. The best fit equation was determined by the differential form of the rate equations and the parameters to determine if the sorption of dyestuffs onto chitosan could be represented in terms of reaction kinetic models.

EXPERIMENTAL

Adsorbent

The adsorbent used in this research was a powdered form of chitin purchased from Sigma Chemical Co. (St. Louis, MO). This chitin was described by the supplier as a practical-grade material extracted from crab shells. All raw chitin was dried at 75°C in an oven for 6 h and then was sieved into a discrete particle size range of 125–500 μm.

Adsorbates

Five different commercially available textile dyestuffs were used in this study, including four azo dyes (AO10, AO12, AR18, and AR73) and one anthraquinone dye (AG25). These selected dyestuffs are commonly used in dye houses nowadays and are regarded as dye contaminants in discharged effluents. All dyestuffs were purchased from Aldrich Chemical Co. (Milwaukee, WI) and were used without any further purification. The characteristics and chemical structures of the selected dyestuffs are listed in Table I and Figure 1, respectively.

Preparation of chitosan

The sieved chitin was deacetylated into chitosan with a 48% sodium hydroxide solution (w/w) at 100°C under a nitrogen atmosphere for 1-h periods. Then, the products were washed with deionized water completely, dried at 70°C in an oven overnight, and sieved again into several particle size ranges (125–250, 250–355, and 355–500 μm). The fractions were further dried in a vacuum oven for 1 day and stored in a desiccator. The degree of deacetylation (DD) of chitosan was characterized by the ^{1}H-NMR method and was found to be 53%.

Concentration measurement and calibration

To calculate the concentration of the sample from each experiment, we first prepared a calibration curve of

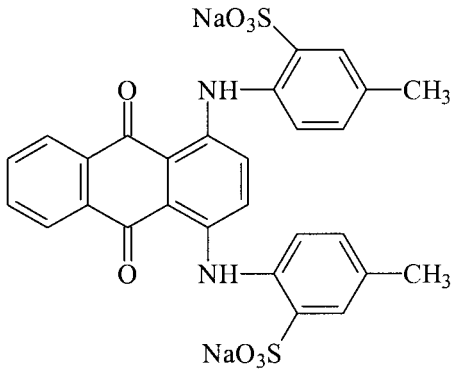

C. I. Acid Green 25 (AG25)

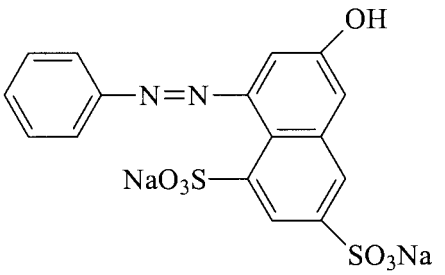

C. I. Acid Orange 10 (AO10)

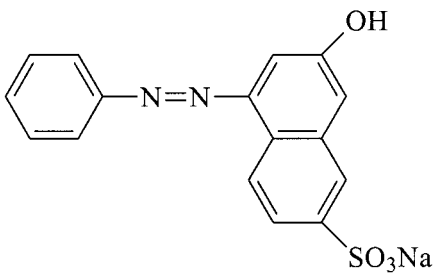

C. I. Acid Orange 12 (AO12)

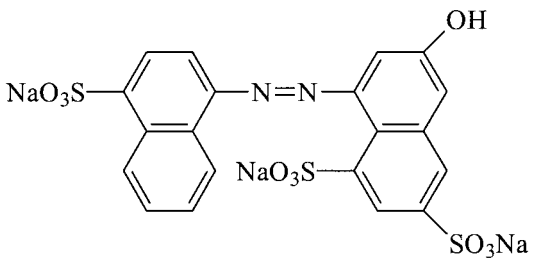

C. I. Acid Red 18 (AR18)

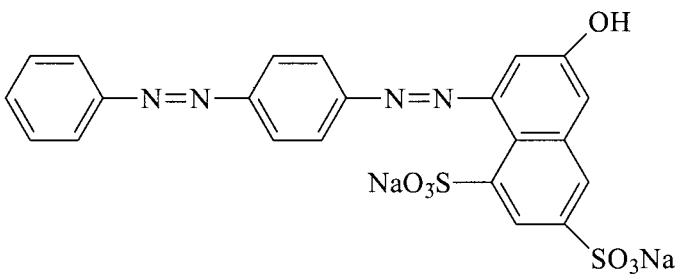

C. I. Acid Red 73 (AR73)

Figure 1 Molecular structures of the five selected dyestuffs.

each dye. For each dye, five different concentrations were prepared, and the absorbance was measured with a PerkinElmer Lambda 18 ultraviolet–visible (UV–vis) spectrophotometer (Norwalk, CT) from 400 to 700 nm. The calibration checks were carried out twice. Then, the maximum absorbance of each dye was plotted with the concentration.

From these results, the concentrations of the dye samples were calculated with the following equations and constants, which are summarized in Table II:

TABLE II
Constant (*k*) for the Calculations of the Dye Concentrations of Selected Dyes

Dye	*k*
AG25	16.650
AO10	22.019
AO12	23.098
AR18	25.928
AR73	40.907

AG25 Dye concentration (mmol/L)

$$= \text{Maximum absorbance}/k_{AG25} \quad (1)$$

AO10 Dye concentration (mmol/L)

$$= \text{Maximum absorbance}/k_{AO10} \quad (2)$$

AO12 Dye concentration (mmol/L)

$$= \text{Maximum absorbance}/k_{AO12} \quad (3)$$

AR18 Dye concentration (mmol/L)

$$= \text{Maximum absorbance}/k_{AR18} \quad (4)$$

AR73 Dye concentration (mmol/L)

$$= \text{Maximum absorbance}/k_{AR73} \quad (5)$$

Equilibrium sorption studies

A fixed mass of chitosan (DD = 53%, 0.2000 g) was weighed into 120-mL conical flasks and brought into contact with 100-mL dye solutions with predetermined initial dye concentrations. The initial pH of the solutions was adjusted to 4.00 ± 0.1 through the addition of a 20 vol % citric acid buffer made up of citric acid and sodium hydroxide. The flasks were sealed and agitated for 24 h at 200 rpm in a thermostatic shaker bath and maintained at a temperature of 25 ± 1°C until equilibrium was reached. At time $t = 0$ and equilibrium, the dye concentrations of the solutions were measured with a UV–vis spectrometer. These data were used to calculate the equilibrium adsorption capacity (q_e) of the adsorbent. Finally, q_e was plotted against the equilibrium concentration (C_e).

Batch-contact-time studies

These sets of experiments were used to investigate the influence of the sorbent mass, the initial concentration, and the particle size of the adsorbent on the adsorption rate. An adsorber vessel in a standard batch stirred tank configuration was used in all the experiments.

Construction of the adsorption vessel

The standard tank configuration was used to derive the relative dimensions of the vessel and its components.[17] The relationships with respect to the inner vessel diameter (D_i) are shown in Figure 2.

A 2-L plastic beaker (internal diameter = 0.13 m) holding 1.7 L of a dye solution was used as the adsorber vessel. Mixing was provided by a six-bladed, flat plastic impeller 0.065 m in diameter with a blade height of 0.013 m. A Heidolph variable motor (Schwabach, Germany) was used to drive the impeller with a 0.005-m-diameter plastic shaft. Six plastic baffles were evenly spaced around the circumference of the vessel, positioned at 60° intervals and held securely in place on top of the vessel. The baffles prevented the formation of a vortex and the consequential reduction in relative motion, between liquid and solid particles, and power losses due to air entrainment at the impeller. The polystyrene baffles were 0.2 m long and 0.01 m wide. They were secured at a position slightly away from the vessel wall and bottom of the tank to prevent particle accumulation.

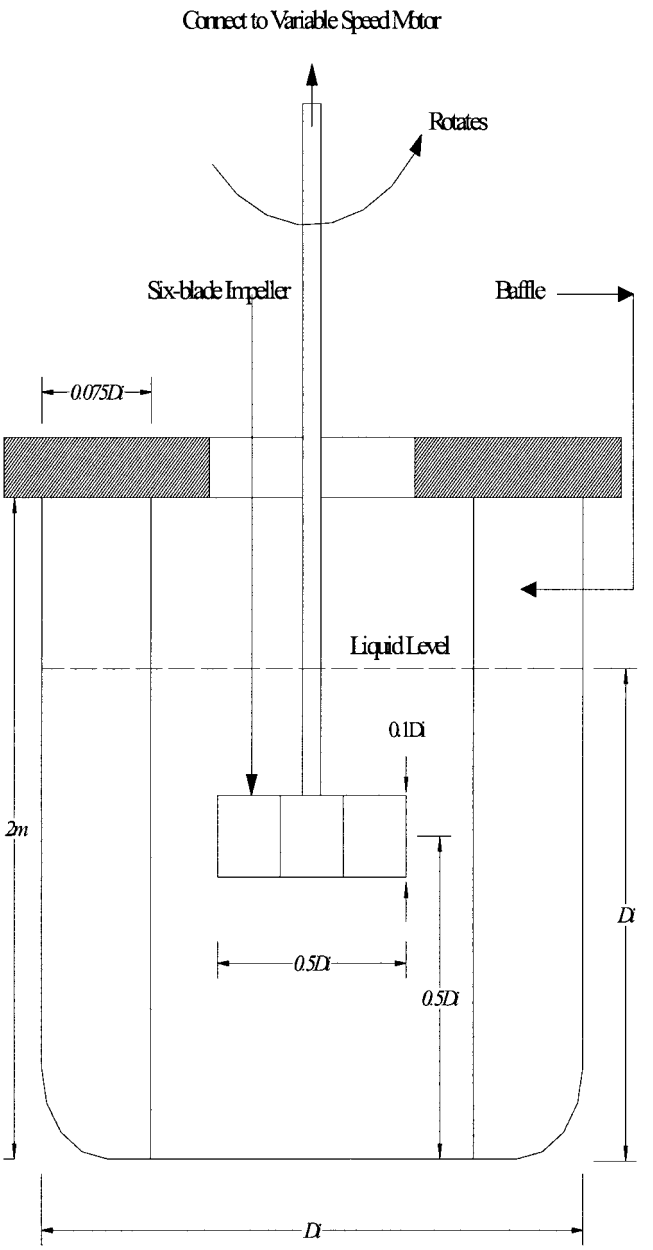

Figure 2 Standard tank configuration for batch-contact-time studies.

Kinetic experiments on various dyes

The adsorption vessel was used to obtain kinetic data, and the following variable parameters were studied.

Effect of the initial dye concentration

We studied the effect of the initial dye concentration on the adsorption rate by contacting a fixed mass of chitosan (1.700 g) at a fixed particle size (355–500 μm) at a fixed temperature (20 ± 1°C) and pH (4.00) with dye solutions of various initial concentrations (from 0.25 to 2.125 mmol/L, depending on the dye being studied). At time $t = 0$ and at selected time intervals (up to 6 h), adequate volumes of the samples were extracted with a Hamilton 2.50-mL syringe (Reno, NV). The sample concentration was determined with a UV–vis spectrophotometer.

Effect of the sorbent mass

The effect of the chitosan mass on the adsorption rate was studied under the same conditions as before, except that the initial concentration of the solution, which was set at 1.00 or 2.00 mmol/L (depending on the type of dye), and a range of sorbent masses (0.4250, 0.8500, 1.275, 1.7000, and 2.1250 g) were used. The sampling, analysis, and treatment of the results were the same as previously described.

THEORY

Equilibrium modeling

To optimize the design of a sorption system for the removal of dyes, we must establish the most appropriate correlation for the equilibrium curves.

Langmuir isotherm

Langmuir[18] proposed a theory to describe the adsorption of gas molecules onto metal surfaces. The Langmuir adsorption isotherm has been successfully applied to many other real sorption processes of monolayer adsorption. Langmuir's model of adsorption depends on the assumption that intermolecular forces decrease rapidly with distance and consequently predicts the existence of monolayer coverage of the adsorbate at the outer surface of the adsorbent.

Theoretically, the sorbent has a finite capacity for the sorbate. Therefore, a saturation value is reached beyond which no further sorption can take place. The saturated or monolayer (as $C_t \rightarrow \infty$) capacity can be represented as follows:

$$q_e = \frac{K_L C_e}{1 + a_L C_e} \tag{6}$$

where q_e is the solid-phase sorbate concentration at equilibrium (mg/g), C_e is the aqueous-phase sorbate concentration at equilibrium (mg/L), K_L is a Langmuir isotherm constant (L/g), and a_L is another Langmuir isotherm constant (L/mg).

Therefore, a plot of C_e/q_e versus C_e gives a straight line of slope a_L/K_L and intercept $1/K_L$. K_L/a_L gives the theoretical monolayer saturation capacity (Q_0).

Therefore, a linear expression of the Langmuir equation is

$$\frac{C_e}{q_e} = \frac{1}{K_L} + \frac{a_L}{K_L} C_e \tag{7}$$

Freundlich isotherm

The Freundlich[19] equation is an empirical equation used to describe heterogeneous systems; it is characterized by the heterogeneity factor $1/n$. Hence, the empirical equation can be written as follows:

$$q_e = K_F C_e^{1/n} \tag{8}$$

where q_e is the solid-phase sorbate concentration in equilibrium (mg/g), C_e is the liquid-phase sorbate concentration in equilibrium (mg/L), and K_F is the Freundlich constant (L/g). A linear form of the Freundlich expression can be obtained from logarithms of eq. (8):

$$\ln q_e = \ln K_F + \frac{1}{n} \ln C_e \tag{9}$$

Therefore, a plot of $\ln q_e$ versus $\ln C_e$ enables constant K_F and exponent $1/n$ to be determined.

Redlich–peterson isotherm

Redlich and Peterson[20] incorporated three parameters into an empirical isotherm. The Redlich–Peterson isotherm model combines elements from both the Langmuir and Freundlich equations, and the mechanism of adsorption is a hybrid one that does not follow ideal monolayer adsorption:

$$q_e = \frac{K_R C_e}{1 + a_R C_e^{\beta}} \tag{10}$$

where q_e is the solid-phase sorbate concentration in equilibrium (mg/g), C_e is the liquid-phase sorbate concentration in equilibrium (mg/L), K_R is a Redlich–Peterson isotherm constant (L/g), a_R is another Redlich–Peterson isotherm constant (L/mg), and β is an exponent lying between 1 and 0.

Equation (10) can be rearranged as follows:

$$K_R \frac{C_e}{q_e} - 1 = a_R C_e^{\beta} \tag{11}$$

This equation can be converted into a linear form through logarithms:

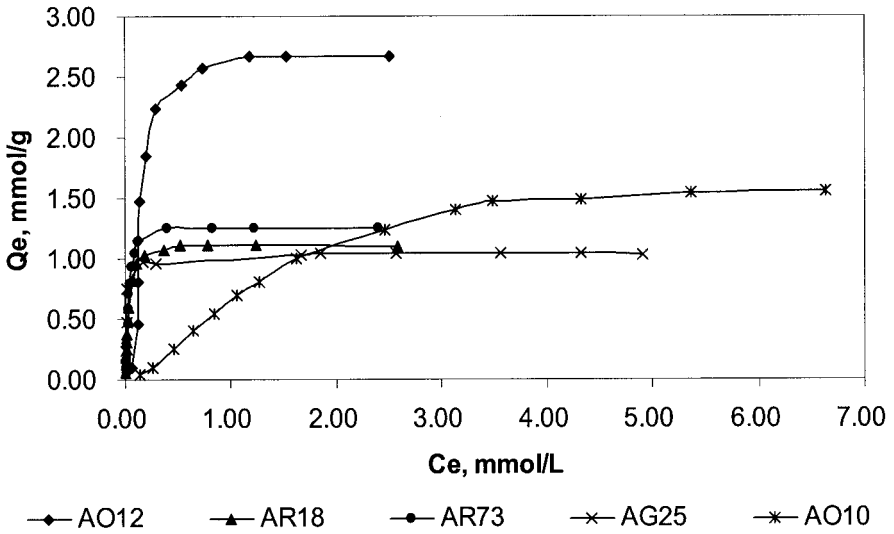

Figure 3 Sorption of acid dyes onto chitosan at 25°C (DD = 53%, pH = 4.00, and discrete particle size = 355–500 μm).

$$\ln\left(K_R \frac{C_e}{q_e} - 1\right) = \ln a_R + \beta \ln C_e \tag{12}$$

Plotting the left-hand side of eq. (12) against ln C_e to obtain the isotherm constants is not applicable because of the three unknowns: a_R, K_R, and β. Therefore, a minimization procedure is adopted to solve eq. (12) by maximizing the correlation coefficient between the theoretical data for q_e predicted from eq. (12) and the experimental data.

Kinetic model

The use of kinetic equations in acid dye sorption has been studied for many years. The mechanism of acid dye sorption onto various sorbents has been subjected to extensive research, debate, and controversy for decades. Much research has been based on a reaction kinetic sorption process in which the reaction rate constants are determined as key parameters describing the process.

Lagergren[21] suggested a pseudo-first-order equation for the sorption of a liquid/solid system based on the solid capacity. The Lagergren equation is the most widely used rate equation in liquid-phase sorption processes, and it can be represented as follows:

$$\frac{dq_t}{d_t} = k_1(q_e - q_t) \tag{13}$$

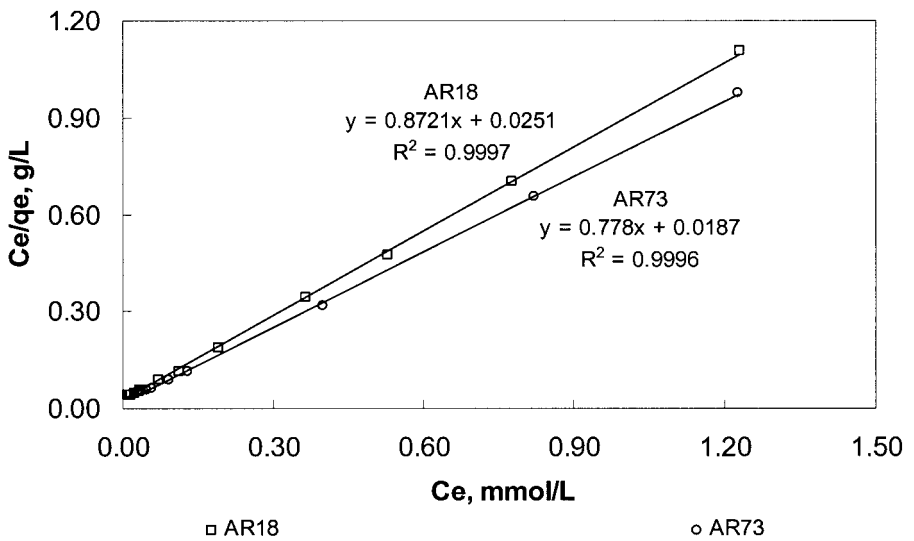

Figure 4 Langmuir isotherm linear plots of the sorption of AR18 and AR73 onto chitosan at 25°C (DD = 53%, pH = 4.00, and discrete particle size = 355–500 μm).

TABLE III
Langmuir Sorption Isotherm Constants for AG25, AO10, AO12, AR18, and AR73

	K_L (L/g)	a_L (L/mmol)	Q_0 (mg/g)	R^2
AG25	175.4390	169.316	645.1	0.9999
AO10	1.1829	0.5798	922.9	0.9812
AO12	33.8983	12.200	973.3	0.999
AR18	39.8406	34.745	693.2	0.9997
AR73	53.4759	41.6043	728.2	0.9996

where q_t is the solid-phase sorbate concentration at time t (mmol/g), q_e is the solid-phase sorbate concentration at equilibrium (mmol/g), and k_1 is a rate constant (h^{-1}).

Integrating this for the boundary conditions $t = 0$ to $t = t$ and $q_t = 0$ to $q_t = q_t$ produces the following:

$$q_t = q_e(1 - e^{-k_1 t}) \tag{14}$$

Equation (14) can be linearized through logarithms:

$$\log(q_e - q_t) = (\log q_e) - \frac{k_1}{2.303} t \tag{15}$$

$$\ln(q_e - q_t) = (\ln q_e) - k_1 t \tag{16}$$

The pseudo-first-order rate constant (k_1) can be correlated by equations of the following form:

$$k_1 = A_1[C_0]^{\beta_1} \tag{17}$$

where C_0 is the initial liquid-phase solute concentration (mmol/L) and A_1 and β_1 are pseudo-first-order constants.

RESULTS AND DISCUSSION

Equilibrium isotherms

Adsorption isotherms describe how adsorbates interact with adsorbents and so are critical in optimizing the use of adsorbents. Therefore, the correlation of equilibrium data by either theoretical or empirical equations is essential to the practical design and operation of adsorption systems. To optimize the design of a sorption system for the removal of dyes from effluents, we must establish the most appropriate correlation for the equilibrium curves. In these studies, the experimental data of five acid dye/chitosan equilibrium isotherms, which were the sorption of AG25, AO10, AO12, AR18, and AR73, as shown in Figure 3, were compared with three isotherm equations: Langmuir, Freundlich, and Redlich–Peterson.

Langmuir isotherm

The Langmuir adsorption isotherm assumes that the adsorbed layer is one molecule thick. The strength of the intermolecular attractive forces is believed to fall off rapidly with distance. The sorption data were analyzed according to the linear form [eq. (7)] of the Langmuir isotherm. The plots of the specific sorption (C_e/q_e) against C_e for five dyes (AG25, AO10, AO12, AR18, and AR73) were carried out, and the data for AR18 and AR73 are shown in Figure 4. The isotherms of AO10, AO12, AG25, AR18, and AR73 were linear over the whole concentration range studied, and the correlation coefficients were extremely high, as shown in Table III. These values of the correlation coefficients strongly support the fact that the dye/chitosan sorption data closely follow the Langmuir model of sorption. The isotherm constants (a_L and K_L) and equilibrium monolayer capacities (Q_0) are presented in Table III.

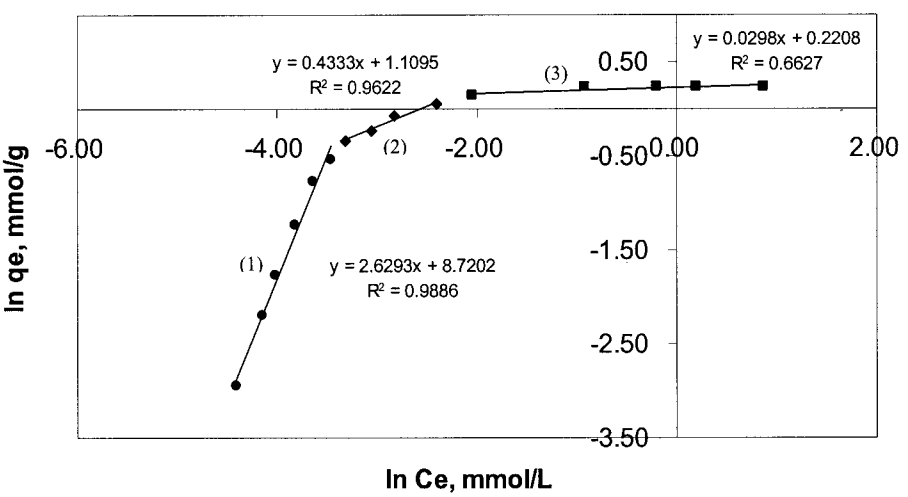

Figure 5 Freundlich isotherm linear plots of the sorption of AR73 onto chitosan at 25°C (DD = 53%, pH = 4.00, and discrete particle size = 355–500 μm).

TABLE IV
Freundlich Sorption Isotherm Constants for AG25, AO10, AO12, AR18, and AR73 at Different Concentration Ranges

Dye	Region	b_F	K_F (mg^3/g)	R^2
AG25	(1)	2.4818	41606	0.9681
	(2)	0.0715	1.0299	0.8508
	(3)	0.0272	1.0046	0.7352
AO10	(1)	1.32	0.651	0.996
	(2)	0.517	0.7755	0.9995
	(3)	0.1105	1.2667	0.9011
AO12	(1)	0.2791	312.249	0.9251
	(2)	0.2324	2.81	0.9199
	(3)	0.027	2.6172	0.577
AR18	(1)	1.087	35.784	0.9957
	(2)	0.4305	2.5053	0.992
	(3)	0.0455	1.1194	0.7874
AR73	(1)	2.6293	6125.4	0.9886
	(2)	0.4333	3.0328	0.9622
	(3)	0.0298	1.2471	0.6627

TABLE V
Redlich–Peterson Sorption Isotherm Constants for AG25, AO10, AO12, AR18, and AR73

	β	K_R (L/g)	a_R (L/mg)	R^2
AG25	0.9963	101.824	98.5366	0.9992
AO10	0.6081	22.435	26.4819	0.9375
AO12	0.9108	25.2658	8.2203	0.9232
AR18	0.9816	38.0287	32.0983	0.9944
AR73	0.9074	1377.996	1119.255	0.9886

The saturation capacities of acid dyes in each of the systems are demonstrated in Figure 3. The saturation capacities of AG25, AO10, AO12, AR18, and AR73 are 1.03, 1.54, 2.66, 1.11, and 1.25 mmol/g, respectively.

The possible mechanisms of the adsorption process of chitosan and acid dye have been examined. In an aqueous solution, the acid dye is first dissolved, and the sulfonate groups of the acid dye (D—SO_3Na) are dissociated and converted into anionic dye ions:

$$\text{D—SO}_3\text{Na} \xrightarrow{\text{H}_2\text{O}} \text{D—SO}_3^- + \text{Na}^+ \qquad (18)$$

Also, in the presence of H^+, the amino groups of chitosan (R—NH_2) are protonated:

$$\text{R—NH}_2 + \text{H}^+ \rightleftharpoons \text{R—NH}_3^+ \qquad (19)$$

The adsorption process then proceeds because of the electrostatic attraction between these two counter ions:

$$\text{R—NH}_3^+ + \text{D—SO}_3^- \rightleftharpoons \text{R—NH}_3^+\text{—}O_3\text{S—D} \qquad (20)$$

Therefore, the differences in the degree of adsorption may mainly be attributed to the chemical structure of each dye.

Freundlich isotherm

The Freundlich equation predicts that the dye concentrations on the adsorbent will increase as long as there is an increase in the dye concentration in the liquid. By plotting the linear transformation of the Freundlich equation, Figure 5 shows the logarithmic plot of the Freundlich expression for the selected acid dye, AR73. A deviation from linearity on the Freundlich linear plot for the whole concentration range for all the dyes can be observed. However, the Freundlich plot may be divided into a number of linear sections, each depict-

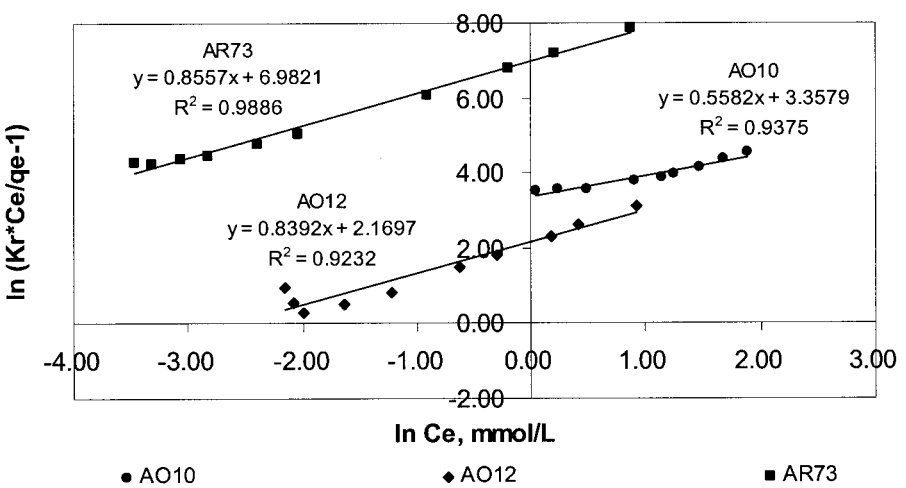

Figure 6 Redlich–Peterson isotherm linear plots of the sorption of AO10, AO12, and AR73 onto chitosan at 25°C (DD = 53%, pH = 4.00, and discrete particle size = 355–500 μm).

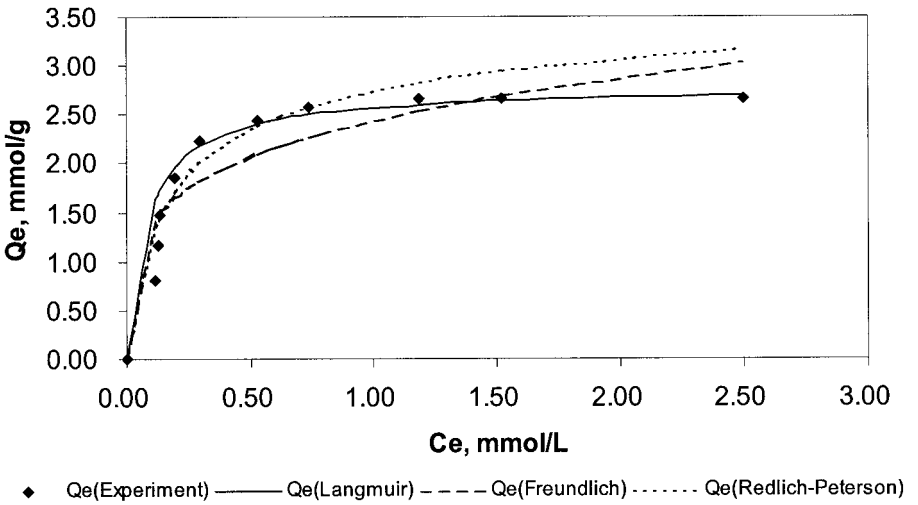

Figure 7 Different isotherm equation plots for the sorption of AO12 onto chitosan at 25°C (DD = 53%, pH = 4.00, and discrete particle size = 355–500 μm).

ing a certain energy range or mechanistic range. Therefore, the whole concentration range is divided into regions, that is, regions 1–3, and excellent fits to the experimental data can be observed, especially at the lower concentration regions (1 and 2). Region 3 does not fit the Freundlich equation well. Table IV shows the Freundlich sorption isotherm constants, b_F and K_F, and the correlation coefficient, R^2, for the different concentration regions.

Redlich–peterson isotherm

The Redlich–Peterson isotherm contains three parameters, and the isotherm equation includes features of the Langmuir and Freundlich isotherm equations. The parameters of the Langmuir and Freundlich models can be determined with the linear forms of the equations. However, the parameters of the Redlich–Peterson isotherms cannot be determined by linearization because these three parameter model equations cannot be solved from the linear equation. Therefore, the parameters of the equations were determined through the minimization of the distance between the experimental data points and the theoretical model predictions with the solver add-in function of Microsoft Excel.

The linearized forms of the Redlich–Peterson isotherm plots for the sorption of three of the five dyes onto chitosan are presented in Figure 6. An examination of the data shows that the Redlich–Peterson model describes the sorption of the dyes on chitosan well over the concentration ranges studied. The Redlich–Peterson isotherm constants a_R, K_R, and β and the correlation coefficient R^2 for the Redlich–Peterson isotherm are listed in Table V.

By comparing the results presented in Tables III–V, we find that the Langmuir sorption isotherm can accurately describe the sorption of AG25, AR18, and AR73 onto chitosan in this study and that the experimental sorption data of AO10 can fit the composite

TABLE VI
Parameters of Pseudo-First-Order Equation for the Sorption of AG25, AO10, AO12, AR18, and AR73 onto Chitosan with Different Initial Concentrations at Room Temperature

Concentration effect					
Dye	Concentration (mM)	k_1	q_e	SSE	R^2
AG25	0.51	1.1310	0.4470	0.0079	0.9635
	1.05	1.1738	0.5065	0.0186	0.9432
	1.56	1.2071	0.5623	0.0100	0.9758
	2.11	1.3218	0.6622	0.0226	0.9555
AO10	0.57	7.9765	0.2034	0.0006	0.9423
	0.86	7.2933	0.3361	0.0023	0.9293
	1.14	6.1393	0.4619	0.0023	0.9052
	1.61	5.3418	0.6562	0.0060	0.9038
	2.32	4.2312	0.9127	0.0181	0.8974
AO12	0.36	4.7935	0.3105	0.0005	0.9902
	0.77	1.7583	0.6861	0.0142	0.9711
	1.05	0.9542	0.9328	0.0271	0.9600
	1.55	0.6992	1.1486	0.05070	0.9534
	2.05	0.6760	1.2011	0.0594	0.9496
AR18	0.26	6.9969	0.2544	0.0003	0.9857
	0.51	3.2743	0.4906	0.0049	0.9728
	1.01	1.5337	0.7742	0.0380	0.9443
	1.55	1.3530	0.8113	0.0623	0.9226
	2.06	1.1148	0.9269	0.0487	0.9259
AR73	0.51	2.4393	0.4717	0.0051	0.9629
	0.76	1.3548	0.6778	0.0235	0.9555
	1.03	0.9939	0.7765	0.0414	0.9766
	1.51	0.7716	0.8686	0.0325	0.9848
	2.04	0.7246	0.9697	0.0327	0.9707

Mass = 1.7000 g; DD = 53%; pH = 4.00; discrete particle size = 355–500 μm.

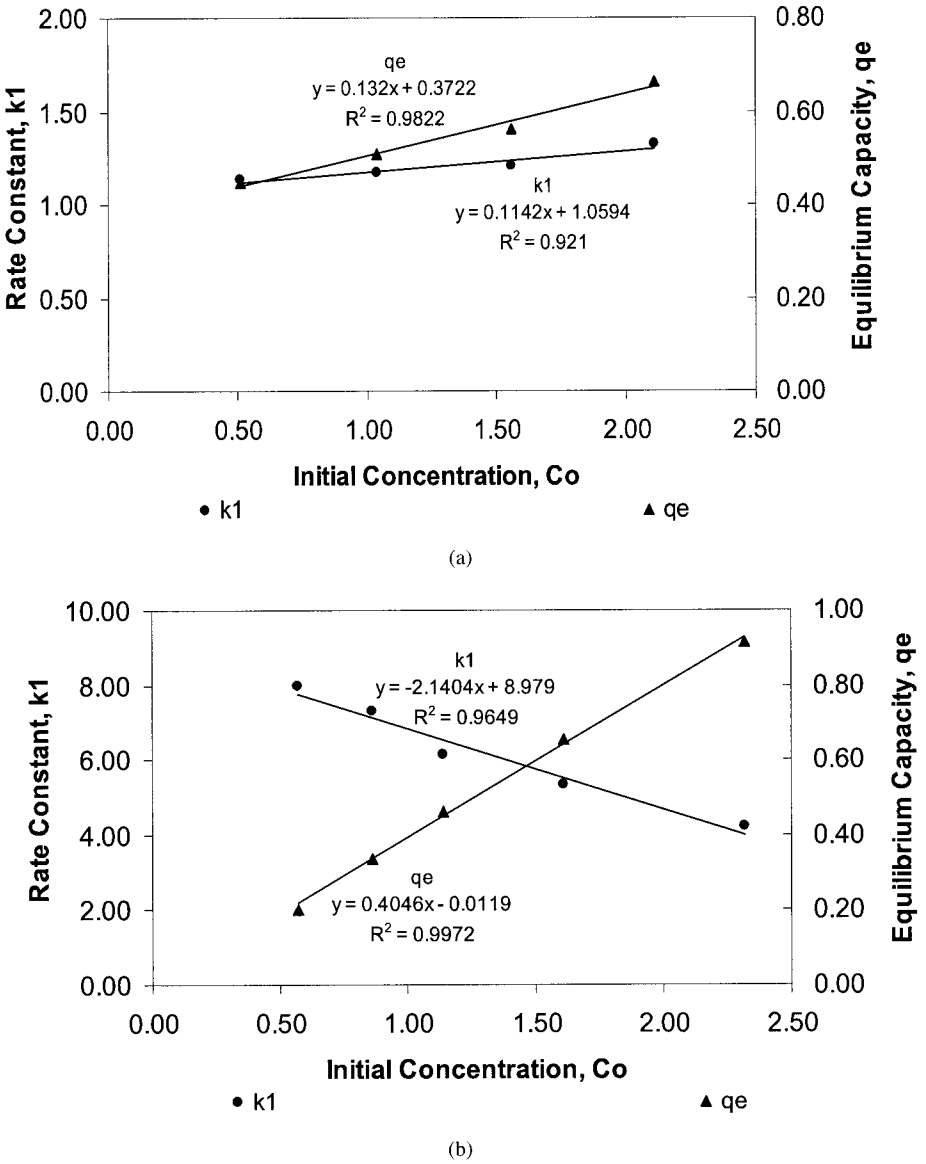

Figure 8 Relationship of the rate constants and equilibrium capacities against the initial concentrations of (a) AG25, (b) AO10, (c) AO12, (d) AR18, and (e) AR73.

Freundlich isotherm model. Figure 7 shows a plot comparing the theoretical Langmuir, Freundlich, and Redlich–Peterson isotherm equations with the experimental data for AO12.

Batch kinetic systems

Sorption systems have been investigated to assess the applicability of chitosan as a suitable sorbent for the removal of acid dyes in dye wastewater. An equilibrium analysis is the most important fundamental study required for evaluating the affinity or capacity of a sorbent. However, an ideal sorbent for wastewater pollution control must have not only a large sorbate capacity but also a fast sorption rate. Therefore, the sorption rate is the other important factor for the selection of the sorbent and sorption kinetics that must be taken into account.

The study of adsorption reaction kinetics is usually assessed in terms of the reaction order of the adsorption process. The experimental results are substituted into the pseudo-first-order kinetic reaction model to determine the sorption kinetic constants by the best fit procedure.

Lagergren equation

Lagergren[21] suggested a first-order reaction equation for the sorption of liquid/solid systems based on the

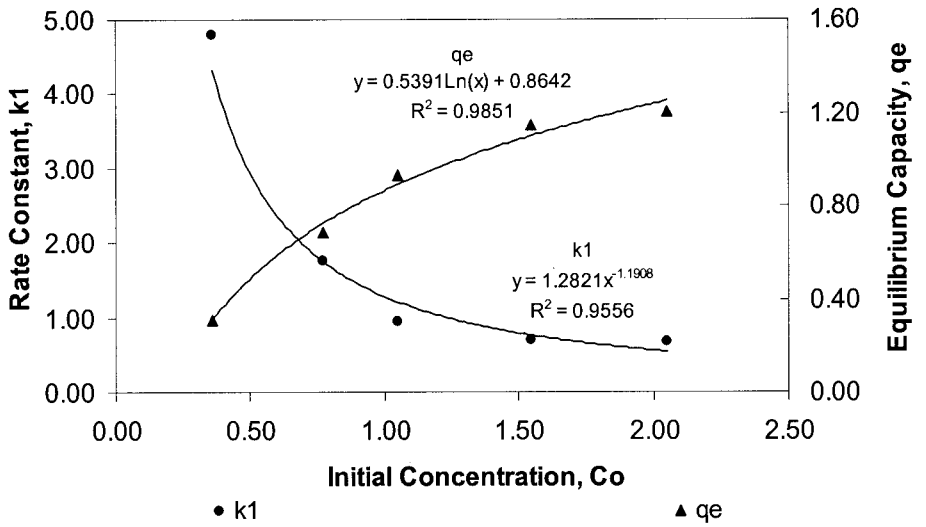

(c)

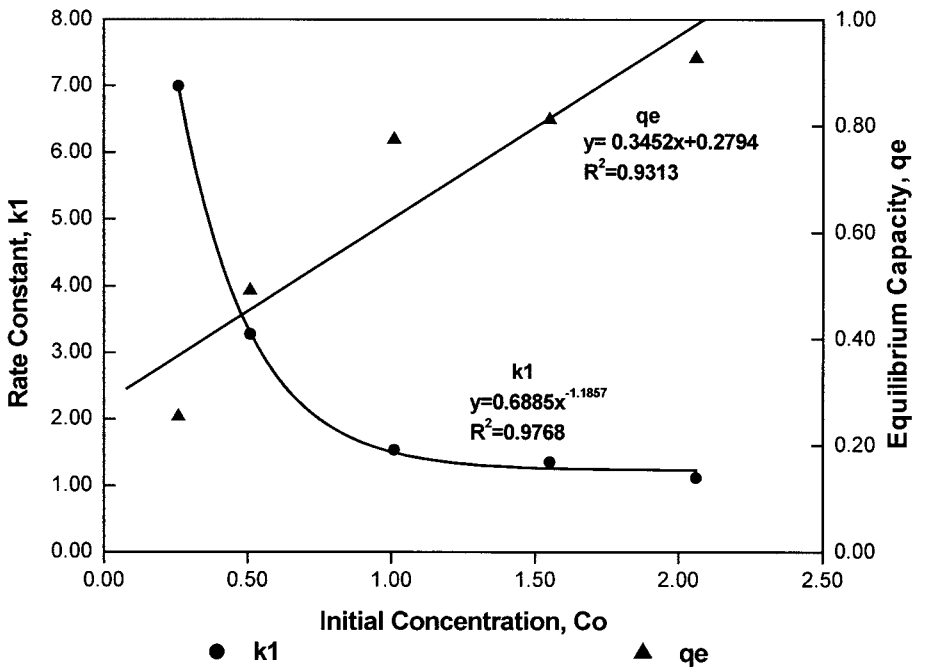

(d)

Figure 8 (*Continued from the previous page*)

solid capacity. This equation has been widely used to define adsorption rates in liquid-phase studies, particularly for the removal of metal ions from effluents and in some cases for the adsorption of dyes. In previous studies, only very limited applications of this pseudo-first-order model have been considered in terms of a range of system variables. These have usually been restricted to one or two initial concentration systems and very few experimental data points.

In this work, the results for five acid dyes were tested with a wide range of initial dye concentrations and different masses of chitosan.

The linear form of the pseudo-first-order equation is shown in eq. (15), where k_1 is the rate constant of adsorption and q_e is the equilibrium capacity of the sorbent. k_1 was calculated from the slope of eq. (15). q_e was calculated by a trial-and-error method in conjunction with an optimization routine to maximize the correlation coefficient for eq. (15) with the solver add-in of Microsoft Excel. R^2 was calculated as follows:

$$R^2 = 1 - \frac{SSE}{SST} \tag{21}$$

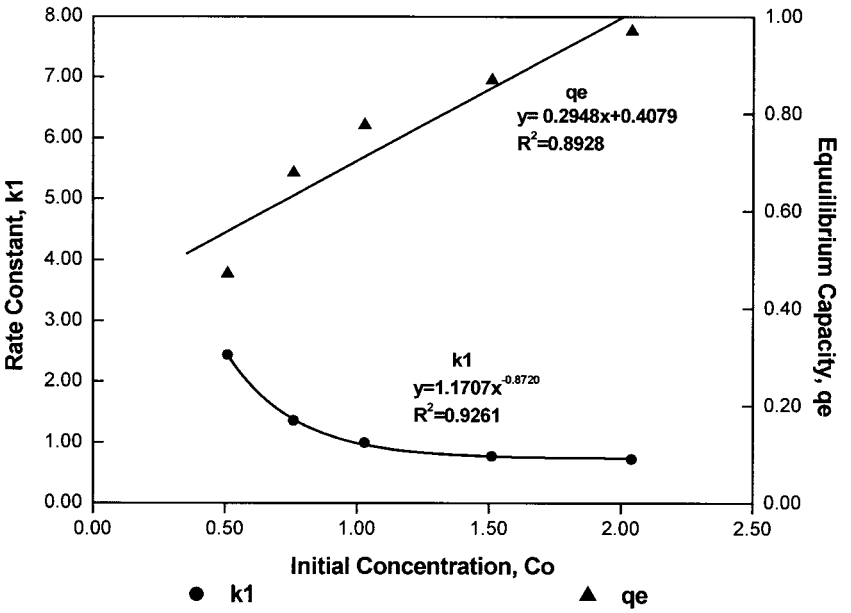

(e)

Figure 8 (*Continued from the previous page*)

where SSE = $\Sigma(q_{exp} - q_{cal})^2$ is the sum of errors squared and SST = $\Sigma(q_{exp})^2 - [(\Sigma q_{exp})^2/n]$ is the sum of total errors squared. k_1 and q_e of each kinetic system were determined by an iterative procedure to obtain the highest value of R^2. Table VI lists k_1, q_e, SSE, and R^2 values for the first-order equation with different initial concentrations of the various acid dyes and different masses of chitosan during the first 3 h of the sorption period. However, the equilibrium capacities of various acid dyes obtained by the solver add-in could not be applied to the later stages of the sorption process, that is, after 3 h of the sorption period; the sorption kinetics at the later stages apparently could involve diffusion kinetics, other reaction kinetics, or their combinations, which could not be correlated well with the pseudo-first-order equation.

The parameters of the rate constant and equilibrium capacity for the sorption of the acid dyes onto chitosan in the pseudo-first-order equation were established. The relationship of the rate constants and equilibrium capacities against the initial concentrations of the solutions is shown in Figure 8(a–e).

The rate constants against the change of the initial concentration of the solutions were best fitted to the equation-of-power function:

$$k_1 = A_1[C_0]^{B_1} \tag{22}$$

Linear equations were used to fit the equilibrium capacities against the change in the initial concentration:

$$q_e = D_1 \ln[C_0] + E_1 \tag{23}$$

The correlations of the parameters are shown in Table VII.

CONCLUSIONS

The performance of chitosan as an adsorbent to remove acid dyes (AG25, AO10, AO12, AR18, and

TABLE VII
Parameters of Pseudo-First-Order Equation for the Sorption of AG25, AO12, AR18, and AR73 onto Chitosan with Different Masses at Room Temperature

	Mass effect				
	Mass of sorbent (g)	k_1	q_e	SSE	R^2
AG25	0.4250	0.6607	0.6408	0.0237	0.9539
	0.8500	0.7858	0.6270	0.0258	0.9474
	1.2750	1.2406	0.5161	0.0062	0.9875
	1.7000	1.5390	0.4512	0.0127	0.9680
	2.1250	1.2336	0.4825	0.0055	0.9869
AO12	0.8500	0.6809	1.4478	0.0305	0.9848
	1.2750	0.7036	1.2694	0.0671	0.9516
	1.7000	0.6760	1.2011	0.0594	0.8995
	2.1250	0.6811	1.1389	0.0468	0.9586
AR18	0.8500	1.4546	0.8919	0.0376	0.9274
	1.2750	1.2868	0.8687	0.0307	0.9418
	1.7000	1.1148	0.9269	0.0487	0.9258
	2.1250	1.2532	0.8671	0.0343	0.9355
AR73	0.4250	0.7122	0.9816	0.0346	0.9800
	0.8500	0.7733	0.9765	0.0291	0.9770
	1.2750	0.8291	0.9261	0.0402	0.9936
	1.7000	0.9939	0.7765	0.0414	0.9840
	2.1250	1.1954	0.7613	0.0227	0.9911

DD = 53%; pH = 4.00; discrete particle size = 355–500 μm.

AR73) from aqueous solutions was investigated. Equilibrium isotherms and kinetic experimental studies were measured and analyzed for the sorption process.

The experimental isotherm data were analyzed with Langmuir, Freundlich, and Redlich–Peterson equations for each individual dye. Based on the Langmuir isotherm analysis, the monolayer adsorption capacities were determined to be 645.1, 922.9, 973.3, 693.2, and 728.2 mg/g of chitosan for AG25, AO10, AO12, AR18, and AR73, respectively. The difference in the capacities may have been due to the difference in the molecular size of the dye molecules and the number of sulfonate groups of each dye. The results demonstrated that the monovalent and smaller dye particles had superior capacities because of the increase in the dye/chitosan ratio in the system, enabling a deeper penetration of dye molecules into the internal pore structure of chitosan. By comparing the correlation coefficients determined for each linear transformation of the isotherm analysis, we found that the Langmuir isotherm equation provided the best overall prediction for the sorption of all five acid dyes for the entire concentration range.

A series of kinetic experiments were carried out and analyzed with the pseudo-first-order reaction kinetic model. The model correlated the experimental data well, particularly at short times of up to 25% of the adsorption process and even up to 60% in most cases. The pseudo rate constants were correlated with the system parameters.

References

1. Marc, R. C&EN Northeast News Bur 1996, 10.
2. Cooper, P. J Soc Dye Colour 1993, 109, 97.
3. Tunay, O.; Kabdasli, I.; Eremektar, G.; Orhon, D. Water Sci Technol 1996, 34, 9.
4. Vandevivere, P. C.; Bianchi, R.; Verstraete, W. J Chem Technol Biotechnol 1998, 72, 289.
5. Okieimen, F. E.; Okundia, E. U.; Ogbeifun, D. E. J Chem Technol Biotechnol 1991, 51, 97.
6. Marshall, W. E.; Champagne, E. T.; Evans, W. J. J Environ Sci Health Part A 1993, 28, 1977.
7. Marshall, W. E.; Johns, M. M. J Chem Technol Biotechnol 1996, 66, 192.
8. Asfour, H. M.; Nassar, M. M.; Fadali, O. A.; Elgeundi, M. S. J Chem Technol Biotechnol 1985, 35, 28.
9. McKay, G.; Elgeundi, M.; Nassar, M. M. Water Res 1987, 21, 1513.
10. Marshall, W. E.; Champagne, E. T. J Environ Sci Health Part A 1995, 30, 241.
11. Cheremisinoff, P. N. Handbook of Water and Waste Treatment Technology; Marcel Dekker: New York, 1995.
12. Allen, S.; Brown, P.; McKay, G.; Flynn, O. J Chem Technol Biotechnol 1992, 54, 271.
13. McKay, G.; Porter, J. F. J Chem Technol Biotechnol 1997, 69, 309.
14. McKay, G.; Otterburn, M. S.; Aga, J. A. Water Air Soil Pollut 1985, 24, 307.
15. McKay, G.; Ramprasad, G.; Mowli, P. P. Water Air Soil Pollut 1986, 29, 273.
16. El-Geundi, M. S. Water Res 1991, 25, 271.
17. Furusawa, T.; Smith, J. M. Ind Chem Eng Fundam 1973, 12, 197.
18. Langmuir, I. J Am Chem Soc 1918, 40, 1361.
19. Freundlich, H. M. F. Z Phys Chem 1906, 57, 385.
20. Redlich, O.; Peterson, D. L. J Phys Chem 1959, 63, 1024.
21. Lagergren, S. Kung Sven Veten Hand 1898, 24, 1.